Assignment of Vibrational Spectra of 1,10-Phenanthroline by Comparison with Frequencies and Raman Intensities from Density Functional Calculations

Markus Reiher,*,† Georg Brehm, and Siegfried Schneider*

Institut für Physikalische und Theoretische Chemie, Universität Erlangen-Nürnberg, Egerlandstrasse 3, D-91058 Erlangen, Germany

Received: September 2, 2003; In Final Form: November 25, 2003

NIR−FT-Raman spectra of 1,10-phenanthroline were recorded of crystalline material and three different solutions (CD_3OD, $CHCl_3$, and CS_2) in the wavenumber range 100−1800 cm^{-1}. FT-IR spectra of the solid material were obtained for the range 400−1800 cm^{-1}. A complete assignment of the experimental vibrational spectra (IR and Raman) of 1,10-phenanthroline is given on the basis of calculated frequencies and Raman intensities obtained from the DFT(BP86) harmonic force field. A satisfactory agreement of the *harmonic* BP86 wavenumbers with the *fundamental* experimental ones is found. This good agreement is due to a systematic error compensation for BP86 harmonic force fields. Raman intensities were calculated within the double harmonic approximation with different basis sets in order to investigate whether moderately sized triple-ζ basis sets with comparatively few polarization functions can properly describe nonresonant Raman scattering. A satisfactory agreement with experimental data for all in-plane vibrations is already obtained with a standard valence triple-ζ basis plus polarization functions. However, for out-of-plane modes, we found a pronounced dependence of frequencies and intensities on the basis set size, which can be well understood by comparison with the results obtained with a larger basis set. The Sadlej basis set, which is recommended for the calculation of electrical properties, leads to deviations of up to 90 cm^{-1} for out-of-plane vibrations. Since 1,10-phenanthroline is hygroscopic and can hardly be obtained in water-free form, particular attention is paid to the influence of bound solvent molecules, like water and methanol, on the vibrational spectrum. Model systems with single solvent molecules attached to the isolated phenanthroline molecule were studied. It was found that the wavenumber shifts induced are generally small.

1. Introduction

1,10-Phenanthroline (Figure 1) represents one of the most frequently used chelate ligands in inorganic chemistry, but a detailed quantum chemical study of its vibrational spectrum has not yet been carried out. This is somewhat surprising since the molecule is only of moderate size and such an investigation would be of great value for studies on complexes, in which the intra-ligand vibrations of phenanthroline must be clearly identified and separated (if possible) from the rest of the vibrational spectrum. An example for such a case represents the classical spin-crossover complex $Fe(phen)_2(NCS)_2$[1−3] for which a correct determination of all vibrational modes is essential for the calculation of the vibrational contribution to the entropy change upon spin flip[4−9] (see also the recent work on other phenanthroline-ligating spin-crossover complexes[10]). There exist numerous other examples, for which the detailed knowledge of intramolecular phenanthroline vibrations is helpful for the assignment of low-frequency vibrations of a metal complex; we refer the reader to the recent work of McGarvey et al.[11,12] on ruthenium complexes, which bind to DNA, and to the investigation by Zgierski[13] on the 2,9-dimethyl-1,10-phenanthroline complex with Cu(I).

Perkampus and Rother recorded the first Raman spectrum of 1,10-phenanthroline, and of other phenanthroline isomers, in the solid state (IR spectra in solution and in the solid state were also recorded).[14] In a subsequent work, Altmann and Perkampus carried out a normal coordinate analysis in combination with the calculation of a classical force field in order to provide an additional means for the assignment of bands in the experimental spectra.[15] A study of per-deuterated phenanthroline isomers was carried out by Thornton and Watkins.[16] They reconsidered the assignment of Perkampus and collaborators and found four new fundamental vibrations as well as some misassigned bands.

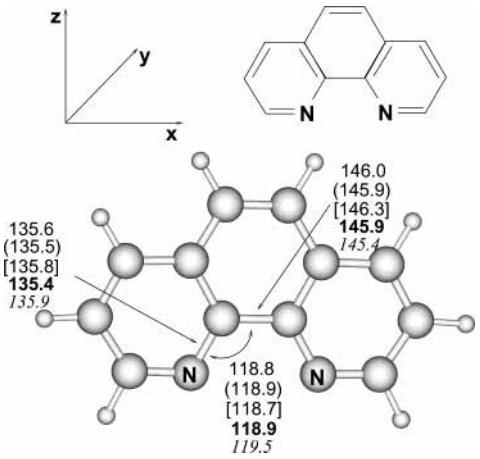

Figure 1. Lewis and BP86 optimized structures of 1,10-phenanthroline in C_{2v} point group symmetry (data: BP86/RI/TZVP, in parentheses BP86/RI/TZVPP, in brackets BP86/Sadlej, in bold face BP86/TZVPPP; the experimental data from ref 43 are given in italics). Distances are given in pm and angles in degrees.

* To whom correspondence should be addressed. E-mail: Markus.Reiher@chemie.uni-erlangen.de. E-mail: Schneider@chemie.uni-erlangen.de.

† Present address: Theoretische Chemie, Universität Bonn, Wegelerstr. 12, D-53115 Bonn, Germany.

10.1021/jp0366116 CCC: $27.50
Published on Web 01/07/2004

Muniz-Miranda[17] gave an almost complete set of (Raman) vibrational frequencies for 1,10-phenanthroline in the solid state, in solution ($CHCl_3$ and H_2O), and adsorbed to silver (using surface-enhanced Raman spectroscopy). In light of the reassigned modes by Thornton and Watkins, Muniz-Miranda provides a new force field. With this force field he also performed frequency calculations and correlated the calculated modes to the original data by Perkampus and Rother. However, in Table 2 of ref 17, the original data by Perkampus and Rother were wrongly quoted. This, in turn, makes the force field data appear in a better agreement with the experimental frequencies. In summary, all normal coordinate analyses applied so far did not originate from a *first-principles* force field as can be provided by quantum chemical methods; instead, empirical force fields have been used for this purpose.

We should also mention that all of these previous studies on vibrational spectra of phenanthroline did not provide enough information on the experimental setup to assess the reliability of bands below about 300 cm^{-1}. We come back to this point later when we consider deviations for the low-frequency vibrations between our measured spectra and the literature data.

Beside the above-mentioned surface-enhanced Raman spectroscopic measurements by Muniz-Miranda, a few other studies also appeared in the literature, where phenanthroline was adsorbed to Ag[18,19] and to Cu.[20] In the latter work by Zawada and Bukowska,[20] spectra of the Cu(I)-phenanthroline complex and the phenanthroline-monohydrate were recorded in order to analyze the frequency shifts upon coordination of phenanthroline to a copper surface.

Apart from the value of a detailed quantum chemical analysis of the phenanthroline vibrational modes for coordination chemistry, the comparatively high symmetry of this molecule should allow us to uniquely assign the experimentally observed bands. This would in turn shed light on the frequency range for which the previously observed remarkable agreement of *harmonic* frequencies from BP86 density functional calculations and *fundamental* experimental ones holds.[21,22] As a valuable spin-off, a correct assignment of vibrational frequencies enables us to compare experimental and quantum chemical Raman intensities in detail. So far, such comparisons have been performed for comparatively small molecules[23−26] and for others with very high symmetry like buckminsterfullerene[27] only. The modeling of the Raman effect requires large basis sets with many polarization functions, which made standard quantum chemical program applications unfeasible. However, within a recently developed methodology,[27] such calculations can easily be carried out, and a detailed comparison of Raman intensities is possible.

In this study, we reexamine all literature data on vibrational frequencies by comparison to those from new, high-resolution measurements and calculations in section 3. Experimental and calculated Raman intensities are compared in section 4. The effect of solvent molecules on the phenanthroline spectrum including intensities is discussed in section 5. The quantum chemical methodology is described in the following section 2.1 and the experimental set up in section 2.2.

2. Quantum Chemical and Experimental Methods

2.1. Quantum Chemical Methodology. For all calculations, the density functional programs provided by the TURBOMOLE 5.1 suite[28] were used. We employed the pure density functional by Becke and by Perdew dubbed BP86[29,30] as implemented in TURBOMOLE. All results are obtained from all-electron restricted Kohn−Sham calculations. Different valence triple-ζ basis sets were used for the calculation of the complete set of Raman intensities: (i) the TZVP basis set[31] features a valence triple-ζ basis set with polarization functions on all atoms, (ii) the TZVPP basis set implemented in TURBOMOLE uses Ahlrichs' TZV core[31] and additional polarization functions taken from the cc-pVTZ basis by Dunning,[32−34] and finally (iii) the Sadlej basis set,[35,36] which is well established as a moderately sized basis set particularly suitable for the calculation of molecular electric properties.[23,37−40] For the BP86/TZVP and BP86/TZVPP calculations, we applied the resolution-of-the-identity (RI) technique[41,42] in order to increase the efficiency of the calculations. Owing to missing auxiliary basis sets for Sadlej's basis set, we did not apply the RI technique for these calculations.

For the out-of-plane vibrations in phenanthroline, it was necessary to use even larger basis sets for accurate harmonic frequencies. Therefore, we also carried out calculations with the TZVPPP basis set from the TURBOMOLE basis set library. All Ahlrichs-type basis sets possess the same TZV kernel, which consists of 11s6p functions for C and N contracted to 5s3p (according to [62111/411]) and of 5s functions contracted to 3s for H (according to the scheme [311]). Although the TZVP basis set possesses an additional d polarization function for C and N and one p function for H, the TZVPP basis set contains two uncontracted d and one f function for C and N and two uncontracted p and one d function for H. The quality of Sadlej's triple-ζ basis set is 10s6p4d contracted to 5s3p2d (according to [52111/411/22]) for C and N and 6s4p contracted to 3s2p (according to [411/22]) for H. The TZVPPP is significantly larger than these three basis sets: it features, in addition to the TZV core, for C and N three uncontracted d functions, two uncontracted f, and one g function and for H three uncontracted p, two uncontracted d and one f function.

Though the Sadlej basis set is the recommended basis set[23,37−40] for the calculation of electric properties, this is not necessarily the case for the calculation of frequencies.[27] Therefore, we aim to elucidate whether the TZVP(P) basis sets can serve as a reliable compromise for calculations of Raman intensities of moderately sized molecules, because they give accurate molecular structures and frequencies. In general, all basis sets, which we use, give excellent molecular structures for 1,10-phenanthroline when compared with the experimental X-ray structure from ref 43 (see Figure 1).

For the frequency analyses, the program package SNF[27] was employed. The second derivatives of the total electronic energy of the harmonic force field are calculated numerically from analytic energy gradients of distorted structures, which were obtained from TURBOMOLE. According to the $O(h^2)$ truncation error of the 3-point central-difference formula used for the first derivative (with a step size $h = 0.01$ bohr), we obtain a four-figure numerical accuracy. The numerical accuracy of the calculated wavenumbers is thus not below 1 cm^{-1}, but we give the first decimal place in order to distinguish the calculated frequencies from the experimental ones in the text. (We do not apply scaling factors for a readjustment of the calculated frequencies.) The IR and Raman intensities are also calculated numerically by using a 3-point central difference formula from dipole moments and *static* polarizabilities, which are obtained from TURBOMOLE calculations (see ref 27 for a detailed description of these techniques). Owing to an error compensation of the currently available approximate density functional methods, *static* polarizabilities yield Raman intensities, which are in better agreement with experiment than those calculated from *dynamic* polarizabilities.[26]

We refrain from giving the calculated IR intensities for several reasons. On one hand, we found a larger basis set dependence

of the IR intensities when compared with results for the Raman intensities. On the other hand, more information on vibrational modes is obtained from Raman intensities owing to the possibility to make use of polarization effects more easily. Although the accuracy of IR intensities obtained with DFT methods was extensively studied,[44] this is not the case for calculated Raman spectra. Therefore, one central aim of this study is to compare calculated and experimental Raman intensities for a molecule of moderate size.

Theoretically determined Raman intensities are often given in terms of Raman scattering factors S_k for a mode k

$$S_k = 45a_k'^2 + 7\gamma_k'^2 \tag{1}$$

where a_k' and γ_k' contain the derivatives $(\bar{\alpha}_{ij}')_k$ (cf. refs 27 and 45):

$$a_k' = \frac{1}{3}\{(\bar{\alpha}_{xx}')_k + (\bar{\alpha}_{yy}')_k + (\bar{\alpha}_{zz}')_k\} \tag{2}$$

$$\gamma_k'^2 = \frac{1}{2}\{[(\bar{\alpha}_{xx}')_k - (\bar{\alpha}_{yy}')_k]^2 + [(\bar{\alpha}_{yy}')_k - (\bar{\alpha}_{zz}')_k]^2 + [(\bar{\alpha}_{zz}')_k - (\bar{\alpha}_{xx}')_k]^2 + 6[(\bar{\alpha}_{xy}')_k^2 + (\bar{\alpha}_{yz}')_k^2 + (\bar{\alpha}_{zx}')_k^2]\} \tag{3}$$

In the second step, these derivatives are now evaluated by numerical differentiation of the components of the polarizability tensors calculated for the structures displaced along the normal coordinates. For comparison with experimental data, it is necessary to express relative intensities in terms of differential cross sections, because these are proportional to the relative intensities obtained in the experiment. The Q-branch differential cross section for a scattering angle of 0° and an incident light beam which is plane polarized perpendicular to the scattering plane is

$$\frac{d\sigma_k}{d\Omega} = \frac{\pi^2}{\epsilon_0^2}(\tilde{\nu}_{in} - \tilde{\nu}_k)^4 \frac{h}{8\pi^2 c\tilde{\nu}_k}\left(\frac{45a_k'^2 + 7\gamma_k'^2}{45}\right)\frac{1}{1 - \exp[-hc\tilde{\nu}_k/k_B T]} \tag{4}$$

Though the polarizabilities were calculated in the static limit and the Raman activities S_k are thus obtained for these static polarizabilities, the cross sections are affected by the laser wavelength of 1064 nm ($\tilde{\nu}_{in} = 9398.50$ cm^{-1}) entering the frequency prefactor ($\tilde{\nu}_{in} - \tilde{\nu}_k$).[4]

2.2. Experimental Methodology. The Raman spectra were recorded from concentrated solutions of phenanthroline in perdeuteraded methanol (CD_3OD), in $CHCl_3$, and in CS_2. Furthermore, Raman and IR spectra of neat crystals were monitored. Because phenanthroline easily incorporates water, the phenanthroline monohydrate and a phenanthroline purified by sublimation were investigated. Because small fractions of water most likely remained in phenanthroline even after sublimation, we pay special attention to the effect of water on the vibrational spectra. However, by comparison of the four different experimental Raman spectra measured in three solvents and in the solid state, we can unambiguously assign the experimental bands from the very beginning and discuss the effect of water molecules as a small perturbation in section 5.

The measurements were performed with an FT-Raman instrument (Bruker RFS 100/S). The optical arrangement employed 180° backreflection with a variable Glan-Thomson polarizer in the detection path and a fixed polarizer in the excitation path. Three spectra were recorded, one without polarizer in the detection path and two with the polarizer at 0° and 90°, respectively. All measurements were carried out with 800 mW laser power at 1064 nm. The resolution was 2 cm^{-1}, and each individual spectrum is an accumulation of 2000 scans.

The relative scattering cross section were obtained from the experimental spectrum by band deconvolution.

3. Assignment of the Experimentally Observed Bands

For 1,10-phenanthroline, an assignment of the experimentally observed bands is possible owing to the C_{2v} point group symmetry: While a_2, b_1, and b_2 modes are depolarized in the Raman spectrum, the a_1 modes are not. Note the particular choice of coordinate axes in Figure 1, which determines the symmetry labels b_1 and b_2. A different choice of x and y axes as it is also in use in the literature on phenanthroline would exchange these labels. The b_1 and b_2 vibrations in refs 14, 16, and 17 are thus classified as b_2 and b_1, respectively, in this work. We decided for the present choice of the coordinate axes because all in-plane vibrations are denoted by symmetry species with subscript 1, whereas all out-of-plane vibrations belong to symmetry species with subscript 2. This is advantageous for later purposes.

Therefore, *all* a_1 modes can exactly be identified based on their polarization properties. Furthermore, a_2 modes are not IR active and thus possess at most a very weak intensity in the experimental IR spectrum due to symmetry breaking in the solid state. Therefore, the assignment of an a_2 band in the Raman spectrum has to be paralleled by a very weak or vanishing intensity in the IR spectrum. Consequently, even in the case of close lying experimental or calculated frequencies, a_1, a_2, and b_i modes can be distinguished. Furthermore, we found (see below) that the in-plane vibrations a_1 and b_1 are well described by the harmonic BP86 force field so that the b_2 modes can be distinguished from the b_1 modes by comparison with the BP86 frequencies.

A small number of the totally symmetric a_1 vibrational modes of phenanthroline were previously calculated with a different DFT technique,[46] namely, with the B3LYP functional and different scaling factors for different frequency regions as they are recommended for the *harmonic* B3LYP force field (see the recent study in ref 22). We refrain from discussing those results in comparison with our work because they are available only for some vibrations, which are in general in fair agreement (in particular, the low lying frequencies are in excellent agreement).

Table 1 compares frequencies calculated with the TZVP, TZVPP, and Sadlej basis sets and those obtained experimentally. For the a_1 modes, we find that the calculated frequencies deviate by less than 20 cm^{-1}, in many cases by less than 10 cm^{-1}, from the experimental ones. Even at small wavenumbers, we find this good agreement.

By comparison of our results for the low-frequency range with the literature, we detected several artifacts and wrong assignments and were able to give a highly reliable assignment even for the low-frequency bands. In Table 1, all re-assigned wavenumbers from the literature are marked by an asterisk (*) and those bands, which are most likely artifacts, are marked by a question mark.

Thornton and Watkins[16] assigned the band at 203 cm^{-1} to the symmetry species a_1. Based on our experimental results, the corresponding vibration cannot be totally symmetric but should be b_2 symmetric. Furthermore, their assigment of vibrations 5, 6, and 7 is not supported by our unambiguous assignment of all totally symmetric vibrations. The assignment of Thornton and Watkins for the modes 5, 6, and 7 was also adopted by Muniz-Miranda.[17] Apart from these, we also detected

TABLE 1: Assignment of Experimental Frequencies to DFT Results[a]

		$\tilde{\nu}_{calc}$, this work			$\tilde{\nu}_{exp}$, this work					reference					
		BP86/RI TZVP	BP86/RI TZVPP	BP86 Sadlej	R s.s.	R CD_3OD	R $CHCl_3$	R CS_2	IR s.s.	16 IR	16 s.s.	17 $CHCl_3$	17 H_2O	17 s.s.	14 s.s.
1	b_2	99.6	100.4	141.6	123					122	122			123	122*
2	a_2	102.8	103.5	150.1	141									144	
3	b_2	223.3	225.7	270.5						203*					
4	a_2	227.0	233.3	292.5	253					254	253			253	
5	a_1	238.0	231.3	241.3	246		245	241		244*	246*	247*	244*	245*	249*
					241?										
6	a_2	382.6	395.1	454.6	401		401	398		406*	403*	401*	402*	402*	395*
7	a_1	402.4	399.3	412.0	410	411	410	408	411	412*	411*	408*	411*	411*	408
					407										
8	b_2	415.9	424.6	453.5	428										
9	b_3	453.4	457.6	466.8	433					429	426	426	430	427	
10	b_2	462.0	485.9	515.1	461		463			457		461	462	466	466*
11	a_2	488.8	545.7	595.9	498				497	499*				495*	
12	b_1	506.7	506.5	526.0	511	512	512		508	509	509	510	510	508	505
13	a_2	540.3	600.7	629.5	604				606		605	600	605	605	600
14	a_1	545.9	544.5	556.4	551	552	552	551		550	552	549	551	552	550
15	b_1	612.2	612.9	605.7	619				622	624	622	622		622	618*
16	a_2	674.4	789.2	838.8											665*?
17	a_1	694.0	694.2	688.9	706	710	708	704	708	708	711	706	710	711	704?
18	b_2	706.0	737.3	769.1					739		738				
19	b_1	721.7	720.3	726.6					724		724				
20	b_2	741.4	749.0	812.4							779				786*?
21	a_2	777.7	837.9	928.2	812				812	810	809			810	814
22	b_2	810.7	834.5	904.3					839	840	831*				840
23	a_1	844.9	845.5	844.3	854	858	857	855	854	853	856	856	859	855	856
															878?
24	b_1	868.5	870.0	879.2	883		885		883	896		882		882	881
25	a_2	913.5	930.6	1012.0											925
26	b_2	913.5	930.6	994.5											942
27	a_2	923.6	947.4	1065.6					955	956	958	962		960	964
28	b_2	935.9	964.9	1065.0					987	988*	982*				985*
										969?	971?	948?			974?
29	a_2	939.3	968.5	1089.7					996						996
30	b_l	1024.0	1024.0	1019.5					1026?						1026?
31	a_1	1031.3	1030.9	1031.9	1035	1040	1038	1034	1036	1037	1036	1035	1042	1035	1033
					1039										
32	b_1	1062.8	1061.1	1063.8			1079			1079					1075
33	a_1	1082.7	1081.6	1079.5	1092	1099	1097	1096	1092	1092	1096	1095	1099	1097	1092
					1096			1090						1121	
34	b_1	1127.4	1124.3	1113.9	1137				1137	1137	1136	1137	1144	1136	
35	a_1	1139.9	1135.5	1132.3	1143		1138		1143					1142	1140
36	a_1	1188.4	1185.0	1184.7	1186	1188			1186	1186	1187	1185	1187	1187	1180
37	a_1	1208.7	1209.7	1219.4	1204	1203		1196	1204	1207*	1204*	1200*	1204*	1204*	1205
38	b_1	1212.5	1211.5	1214.8	1218	1220			1217	1217*	1218*	1215*	1218*	1218*	1214*
39	b_1	1260.5	1259.1	1248.8	1268	1266	1266	1264	1268		1253	1256		1253	1254
												1264	1265	1263	1262
													1280	1274	
40	a_1	1295.8	1299.7	1314.9	1293	1295	1293	1290	1295	1295	1295	1291	1297	1294	1292
41	b_1	1319.8	1325.1	1347.3		1309	1308	1305	1312	1312	1314	1307		1314	1308
42	a_1	1343.3	1342.9	1341.6	1345	1344	1343	1342	1345	1345	1345	1341	1343	1345	1343
												1376?			1382?
43	a_1	1371.9	1376.6	1392.1	1401	1406	1404	1399		1405*	1405*		1408*	1405*	1404
					1414						1414	1415		1414	
44	b_1	1400.9	1401.1	1392.1	1406	1396	1394	1391	1405						
45	b_1	1409.6	1411.9	1406.4		1421	1417	1410	1422	1422	1420		1420	1420	1417
46	a_1	1435.1	1437.8	1435.9	1448	1451	1450	1447	1447		1446	1448	1451	1446	1444
												1460?			
47	a_1	1486.1	1490.9	1494.5	1503	1508	1507	1502	1503	1502	1502	1505	1512	1502	1505
												1538?		1541?	
48	b_1	1488.3	1488.7	1490.6	1493		1494		1493	1492		1496		1492	1493*
49	b_1	1532.3	1535.5	1545.8	1560	1566	1564	1558	1560	1561	1562	1561	1569	1562	1558
							1586	1583							
50	a_1	1578.8	1580.1	1587.4	1590	1599	1594	1593	1586	1585*	1587*	1592*	1591*	1588*	1586*
51	b_1	1593.4	1594.8	1601.8	1606	1606	1607	1605	1599	1597*	1601*	1605*	1603*	1601*	1599*
52	a_1	1607.6	1606.5	1614.3	1618	1622	1621	1618	1616	1615	1617	1619	1622	1617	1616
53	b_1	3065.9	3064.2	3046.9											3038
54	a_1	3066.2	3065.5	3047.3										3035	3026
55	b_1	3087.7	3086.1	3079.8											
56	a_1	3096.1	3095.1	3086.5										3058	3053
57	b_1	3096.3	3096.5	3088.2											3092
58	a_1	3104.7	3102.4	3101.8										3065	3065
59	a_1	3120.3	3119.9	3110.2										3080	3076
60	b_1	3120.7	3121.6	3109.9											3105

[a] All wavenumbers (given in cm^{-1}) are classified according to the species of C_{2v} point group symmetry. (R = Raman, IR = infra-red, s.s. = solid state, * denotes bands from the literature, which we have re-assigned.)

several other inconsistencies, marked by an asterisk (*) in Table 1. For instance, the comparatively intense IR band at 831 cm^{-1} observed in ref 16 appears to be of b_2 symmetry when compared with our experimental and theoretical results rather than of a_2 symmetry as assigned in ref 16.

Modes 37 (a_1 symmetry) and 38 (b_1 symmetry) appear to have been wrongly assigned (i.e., exchanged) in all previous assignments. In view of the different polarization properties of these different symmetry species and because of the corresponding intensities discussed in the next section, the assignment must be the one given in Table 1. Also, mode numbers 50 and 51 are exchanged in the previous literature assignments when compared with our study. Here, pure symmetry arguments require our assignment of these two vibrations. Apart from these four vibrations, we identify a further inconsistency at wavenumbers above 1000 cm^{-1}: this is mode number 43, which is the most intensive band in the theoretical Raman spectrum and should therefore be clearly identified. However, the wavenumbers given in the refs 16 and 17 deviate by more than 10 cm^{-1} from our and Perkampus' data.[14] It appears that the data given in refs 16 and 17 for this mode is in better agreement with the following mode of b_1 symmetry.

Before we discuss the situation at lower wavenumbers, we should make some remarks on accuracy reached in the quantum chemical calculations. The overall agreement between TZVP and TZVPP data is satisfactory (deviations are usually much smaller than 5 cm^{-1}) and also the Sadlej basis set yields good results though we would have expected a slightly worse performance in view of the results for buckminsterfullerene reported in ref 27. Although the former statement is in particular true for all vibrational modes above 1000 cm^{-1}, we find some significant deviations for the b_2 and a_2 modes, which involve out-of-plane motions. For low-frequency modes of these symmetries, we find large deviations between the results obtained with the three different basis sets. Because this could originate from the step size chosen for the numerical differentiations, we increased the step size for the structure distortions from the standard 0.01 to 0.05 bohr. With this larger step size, most frequencies are changed by less than 3 cm^{-1}, though there are two exceptions. These exceptions are the a_2 modes No. 11 and No. 16, which shift by about 20 cm^{-1} (please note that the data for step size 0.05 bohr are not given in Table 1). However, even shifts of this magnitude are not able to explain the large deviations between the TZVP and TZVPP results for the a_2 modes. We should note that the *harmonic* approximation for the description of the potential energy surface around the equilibrium structure of the system cannot be the reason for the deviating results for the harmonic frequencies calculated either, because upon enlargement of the basis set, these should converge to a limiting value.

Therefore, the reason that the low-frequency b_2 and a_2 modes depend extremely on the basis set size must be their particular type of vibration. These vibrations are all out-of-plane modes. Normal coordinate pictures are presented in Figure 2 for those out-of-plane modes, which are visible in the experimental Raman spectra. To approach the basis set limit of the harmonic frequencies, we performed a frequency analysis with the larger TZVPPP basis set from the TURBOMOLE basis set library. In general, vibrational frequencies obtained with the larger TZVPPP basis set deviate by less than 2 cm^{-1} from the TZVPP results. *All* wavenumbers for out-of-plane vibrations obtained with Sadlej's basis set differ by more than 30 cm^{-1} from the TZVPP results and up to 90 cm^{-1} from the TZVPPP data. The Sadlej basis is thus largely affected by basis set superposition

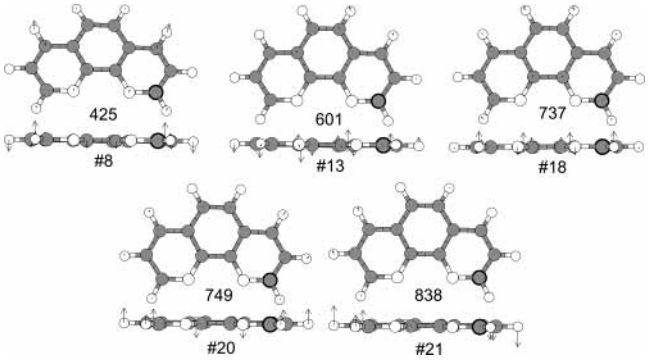

Figure 2. Out-of-plane modes visible in the experimental Raman spectra. The wavenumbers in cm^{-1} are taken from the BP86/RI/TZVPP calculations.

effects in our semi-numerical approach. The smaller TZVP basis set performs much better; differences to the TZVPPP results are generally less than 10 cm^{-1}, but for a few vibrations, they are as large as about 50 cm^{-1}. Since auxiliary basis sets for the RI technique are not available for the TZVPPP basis, we did not employ the RI approximation in the TZVPPP calculation. Because the vibrational frequencies obtained with the TZVP, TZVPP, and TZVPPP basis sets differ only little, the RI approximation can be excluded as a source of errors. Note that the TZVP basis set also provides reliable results for almost all vibrations with a few exceptions, which are all out-of-plane motions.

A comparison of the calculated data for the low-frequency out-of-plane vibrations with experiment reveals that the TZVPP frequencies are in good agreement with the experimental values (occasionally the deviation is up to 25 cm^{-1} but in general it is below this value). One exception is found for mode number 3, where our measured data deviates by about 80 cm^{-1} from our calculated data and by about 100 cm^{-1} from the data given in the literature.

We should mention here that the cited publications do not contain enough details for an assessment of our experimental vibrational frequencies in comparison with the reported ones. In particular, Perkampus and Rother[14] show a vibrational spectrum of 1,10-phenanthroline but do not provide sufficient information on the experimental set up employed for the measurement. Altmann and Perkampus[15] refer to ref 14 without giving additional information on the experimental conditions. On the other hand, Thornton and Watkins[16] do give this information (488 nm incident laser light (100 mW), spinning cell, etc.) but do not depict a vibrational spectrum, from which the quality of the measurements and the unambiguity of the presented wavenumbers could be judged. Only Muniz-Miranda[17] provides sufficient information on the experimental conditions and shows a spectrum recorded from both a solution and from the solid state. Both spectra exhibit a poorer quality in the low-frequency range when compared with our spectra. As alternative reason for the differences observed in the low-frequency range, we will discuss in section 5 environmental effects by solvent molecules.

4. Comparison of Calculated and Experimental Raman Intensities

To provide a first-sight comparison of the BP86/RI/TZVPP Raman spectrum and the experimental Raman spectrum, Figure 3 shows the Gaussian-broadened BP86/RI/TZVPP relative scattering factors and one of the experimentally recorded spectra (solid state).

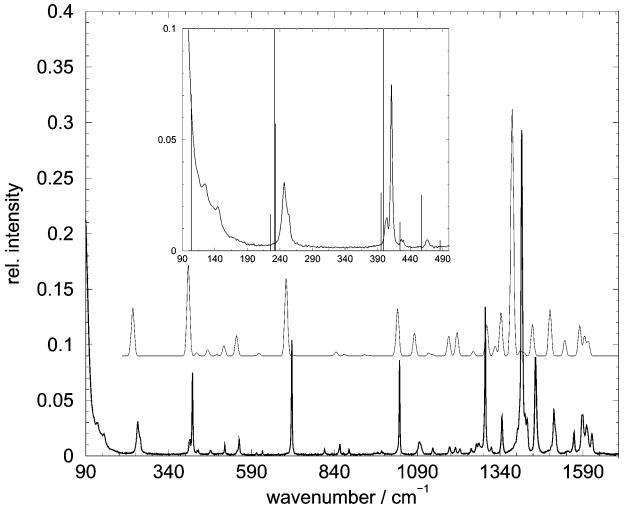

Figure 3. Comparison of the Gaussian-broadened BP86/RI/TZVPP spectrum (shifted upward) with the experimental solid-state Raman spectrum of phenanthroline. The inlay shows a blow-up of the low-frequency experimental spectrum (calculated frequencies and intensities are given as a line spectrum).

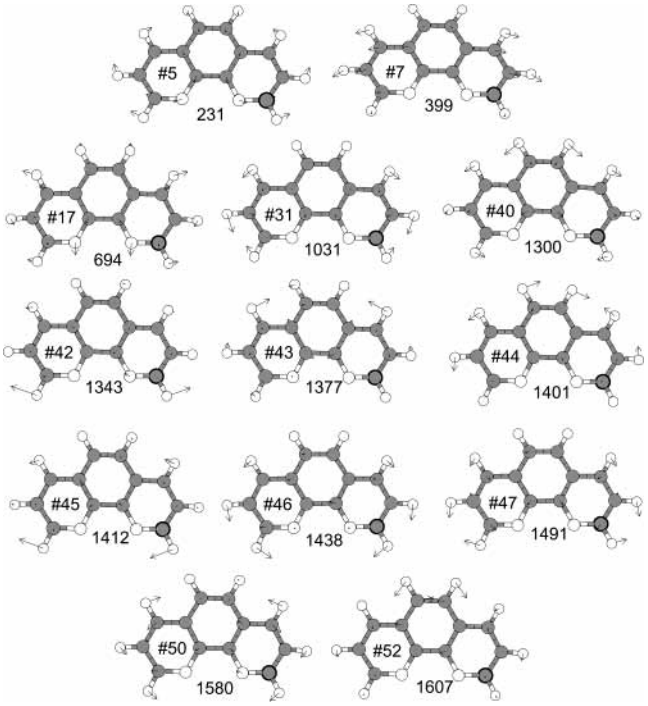

Figure 4. Most intense in-plane modes according to Table 2 with relative experimental scattering cross sections $d\sigma/d\Omega > 0.10$. The wavenumbers in cm^{-1} are taken from the BP86/RI/TZVPP calculations.

Of the 10 modes with highest intensities (see also Figure 4), all except mode numbers 44 and 45 are of a_1 symmetry. This is in accordance with the expectation that the Raman activity is large for "symmetric" modes, i.e., for those modes, which belong to the totally symmetric irreducible representation.

For a detailed comparison of calculated and experimental Raman intensities, we compare the numerical values of Raman activities S_k and relative scattering cross sections $d\sigma_k/d\Omega$ for those vibrational modes, which are visible in the experimental Raman spectrum. From the available experimental Raman spectra, we picked the one, which was measured in $CHCl_3$. The data are given in Table 2. By inspection of Table 2, we see that the TZVP and TZVPP basis sets, which were not optimized for the calculation of optical properties, perform satisfactorily when compared with the Sadlej basis set. The TZV(P,PP) basis sets can thus safely be recommended for the calculation of Raman spectra (in addition to their value for structure optimization and reaction energies). When compared with the experimental data, we find a more than qualitative agreement with the calculated spectrum. This is indeed noteworthy in view of the approximations necessary in the quantum chemical calculations (double harmonic approximation for Raman activities and isolated-molecule calculation).

The most intense Raman mode is No. 43 in the experimental as well as in the calculated spectrum. Though all calculated intense modes above 500 cm^{-1} match the experimental ones, we do not find significant experimental intensities for mode numbers 5 and 7, which should be visible in the experimental spectrum according to the calculations.

5. Effect of Solvent Molecules on Frequencies and Intensities

Phenanthroline is very hygroscopic; each phenanthroline molecule can easily bind one water molecule. To arrive at a consistent picture of the effect of crystal water the vibrational spectrum of 1,10-phenanthroline and that of other solvent molecules (which is already documented in the solvent-dependent wavenumbers presented in Table 1), we discuss in the following the calculated spectra of the monohydrate and of the methanol-monohydrate complex, respectively. These two hydrogen-bonded molecules shall model the complexation of phenanthroline in the monohydrate crystal and in perdeuterated methanolic solution. Though, in general, the modeling of Raman and IR spectra of solvated species is best approached within very computer-resource and time demanding first-principles molecular dynamics simulations, we restrict ourselves in this work on model studies of one-to-one adducts, which reflect the stoichiometric composition of the monohydrate phen·H_2O. The structural and energetical description of such hydrogen-bonded complexes by the standard density functional methods, which we use, can be expected to be sufficiently accurate (see, e.g., refs 47−49). The optimized BP86/RI/TZVPP minimum structures of both complexes are depicted in Figure 5. The electronic binding energy of the water molecule in the water−phenanthroline complex is 29.6 kJ/mol (including a counter-poise correction for the basis set superposition error), whereas we find a binding energy of H_2O to the phenanthroline-methanol complex of 31.6 kJ/mol. The total hydrogen bond energy of water in the methanol complex can be decomposed on the basis of the shared-electron number (SEN) partitioning scheme described in ref 48. We obtained a SEN value of 0.0299 for the H1(water)-O(methanol) pair and a SEN value of 0.0411 for the H2(water)-N(phen) pair of atoms. Accordingly, we attribute 13.3 kJ/mol of the total interaction energy to the H1−O interaction and 18.3 kJ/mol to the H2−N interaction. In view of the BP86/RI interaction energy of the water dimer of about 20 kJ/mol,[48] the hydrogen bonds of water in a complex with phenanthroline are comparatively strong.

For the monohydrate, we find a strong coupling between water and phenanthroline for all modes up to 613 cm^{-1} (i.e., from mode no. 1 to 15) but almost no change of the wavenumber of localized phenanthroline modes upon coupling, only some of these modes show shifts up to 5 cm^{-1} and mode number 2 shifts by 10 cm^{-1}. Apart from vibration number 24, which weakly couples with the water molecule and shifts to 873.5 cm^{-1}, i.e., by 3.5 cm^{-1}, we do not find any further coupling of phenantholine vibrations with those of the water molecules. In the case of our second solvation model, we also find only small

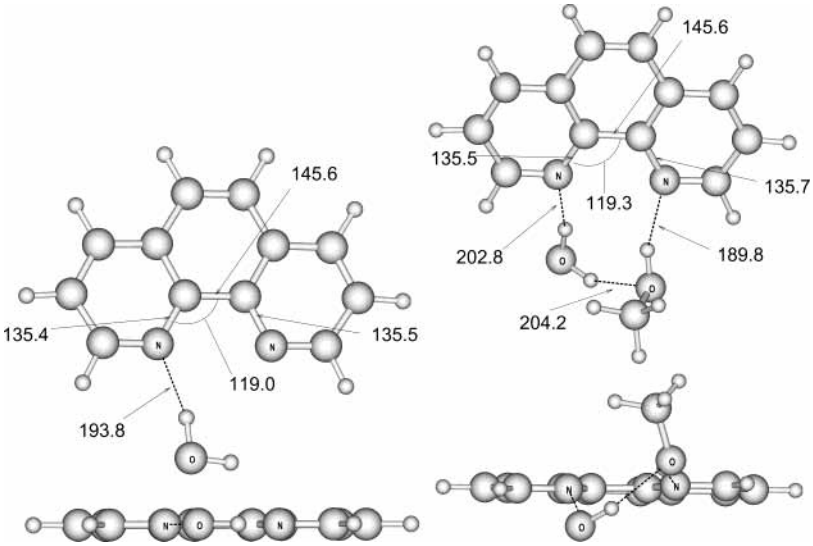

Figure 5. Optimized structures (top and side view) of phenanthroline-monohydrate (left, BP86/RI/TZVPP) and the complex with (perdeuterated) methanol (right, BP86/RI/TZVPP). The distances are given in pm and the angles in degrees.

TABLE 2: Comparison of Raman Activities S_k in Å^4/amu and Relative Scattering Cross Sections $d\sigma_k/d\Omega$ for Those Modes, Which Are Visible in the Experimental Raman Spectrum (Measured in $CHCl_3$)[a]

	BP86/RI/TZVP		BP86/RI/TZVPP		BP86/Sadlej		exp.
mode no.	S_k	$d\sigma_k/d\Omega$	S_k	$d\sigma_k/d\Omega$	S_k	$d\sigma_k/d\Omega$	$d\sigma_k/d\Omega$
2	0.5498	0.0890	0.4433	0.0705	0.6117	0.0646	
3	0.4814	0.0204	0.4044	0.0166	0.2884	0.0113	
4	1.5578	0.0643	1.4774	0.0573	1.2290	0.0426	
5	4.1079	0.1571	3.4231	0.1347	3.7233	0.1760	
6	1.7495	0.0316	1.5473	0.0262	1.1285	0.0199	
7	19.1673	0.3129	21.1205	0.3518	23.1309	0.4733	
8	0.8292	0.0132	0.8597	0.0131	0.7750	0.0137	
9	1.9170	0.0269	1.8561	0.0252	2.5533	0.0434	
12	3.7695	0.0442	3.5356	0.0414	2.2391	0.0320	0.02
14	7.4358	0.0787	6.9916	0.0737	7.2973	0.0960	0.08
17	42.0372	0.3141	42.4091	0.3150	45.6245	0.4410	0.26
23	3.9254	0.0222	2.8627	0.0160	3.7375	0.0269	0.03
24	1.3957	0.0076	1.2490	0.0067	0.8288	0.0056	0.01
30	2.7636	0.0118	2.4524	0.0103	2.3450	0.0127	
31	44.1231	0.1853	45.2470	0.1878	51.2062	0.2732	0.21
32	0.0739	0.0003	0.0436	0.0002	0.1029	0.0005	
33	18.1067	0.0708	23.5872	0.0909	28.3234	0.1410	0.08
34	1.9685	0.0072	3.0697	0.0111	4.5585	0.0216	
35	1.1492	0.0041	1.6881	0.0060	2.3815	0.0110	0.03
36	24.5299	0.0830	24.0113	0.0802	16.9342	0.0728	
37	27.2131	0.0894	24.0104	0.0776	30.7801	0.1264	0.09
38	5.2785	0.0173	5.7405	0.0185	5.4601	0.0226	
39	6.2790	0.0193	5.9366	0.0180	5.1763	0.0204	0.06
40	48.5181	0.1427	43.7803	0.1258	6.5597	0.0238	0.31
41	13.8262	0.0393	14.2334	0.0396	14.6409	0.0510	0.02
42	77.8065	0.2151	64.5799	0.1758	85.6814	0.3007	0.10
43	374.1683	1.0000	383.0867	1.0000	303.3187	1.0000	1.00
44	14.2182	0.0366	8.4139	0.0213	17.4083	0.0574	0.03
45	0.9501	0.0024	5.2583	0.0131	0.4014	0.0013	0.13
46	59.7826	0.1479	52.6399	0.1275	170.6203	0.5334	0.27
47	74.9071	0.1743	77.3109	0.1759	95.3121	0.2779	0.14
48	4.7742	0.0111	5.7645	0.0131	2.8687	0.0084	0.01
49	32.3596	0.0713	29.2521	0.0632	33.7217	0.0926	0.07
50	56.3395	0.1177	59.8149	0.1226	69.2219	0.1812	0.21
51	40.0554	0.0822	39.3726	0.0794	42.5721	0.1096	0.08
52	33.1445	0.0670	29.6459	0.0590	29.6440	0.0752	0.08

[a] The mode numbers are according to the ordering obtained from BP86/RI/TZVP calculations as introduced in Table 1. Vibrations with calculated intensities less than about 1% (exception: those cases in which experimental values are available) and above 3000 cm^{-1} are not given.

shifts of wavenumbers. In the range between 1600 and 1400 cm^{-1}, only the mode with number 49 is shifted by about 11 cm^{-1} from 1535.5 to 1546.7 cm^{-1}. Mode Nos. 31 and 32 couple with C−D bending vibrations and shift by 6 and 16 wavenumbers, respectively. In the low-frequency region, we find a coupling between phenanthroline and water or CD_3OD vibrations, but the wavenumbers are not shifted in many cases. However, the a_1 modes with numbers 5 and 7 are shifted toward larger wavenumbers by 5−11 cm^{-1}. Some selected vibrational frequencies and Raman activities of our solvation models are given in Table 3.

A quantitative analysis of the vibrational mixing of phenan-

TABLE 3: Vibrational BP86/RI/TZVPP Frequencies in cm^{-1}, Raman Activities S_k in $Å^4$/amu of Some Selected Low- and High-Frequency Vibrations in the Hydrogen-Bonded Solvent Complexes of Phenanthroline[a]

mode	phen·monohydrate		phen·[H_2O,CD_3OD]		isolated phen	
no.	$\tilde{\nu}$	S_k	$\tilde{\nu}$	S_k	$\tilde{\nu}$	S_k
3	223.9	0.3277	226.3	0.1657	225.7	0.4044
4	227.7	1.6027	232.1	1.9464	233.3	1.4774
5	233.9	3.3197	242.5	3.0568	231.3	3.4231
6	395.8	1.5566	388.7	1.0690	395.1	1.5473
7	404.5	20.6224	404.2	13.2528	399.3	21.1205
47	1493.6	57.7250	1498.6	48.2076	1490.9	77.3109
50	1580.7	61.6228	1581.0	67.5564	1580.1	59.8149
51	1594.7	40.8817	1595.3	39.9255	1594.8	39.3726
52	1607.2	25.8146	1609.3	26.6675	1606.5	29.6459

[a] Selected data for the isolated phenanthroline molecule from Tables 1 and 2 are given in the last two columns for comparison.

TABLE 4: Quantitative Analysis of the Vibrational Contribution of Pure Phenanthroline Modes in Some Selected Low- and High-Frequency Vibrations in the Hydrogen-Bonded Water-Methanol Solvent Complex of Phenanthroline[a]

i	$\Delta\tilde{\nu}_i$	A^i_{mm}	A^i_{nm}	i	$\Delta\tilde{\nu}_i$	A^i_{mm}	A^i_{nm}
3	0.6	0.99	0.99	47	7.7	1.00	0.91
4	−1.2	0.98	0.77	50	0.9	1.00	0.91
5	11.2	0.98	0.84	51	0.5	1.00	0.91
6	−6.4	0.58	0.70	52	2.8	1.00	0.91
7	4.9	0.92	0.72				

[a] $A^i_{nm} = \langle n_i|\tilde{m}_i\rangle$ corresponds to the fraction of mode n_i contained in the corresponding mode m_i of the hydrogen-bonded complex. For the discussion of the A^i_{mm} and A^i_{nm} see text. The wavenumber shift $\Delta\tilde{\nu}_i$ is given in cm^{-1} (BP86/RI/TZVPP).

throline modes and solvent modes in the two solvation models is possible in terms of a simple normal mode overlap A^i_{nm} calculation

$$A^i_{nm} = \langle \mathbf{n_i}|\tilde{\mathbf{m}}_i\rangle \tag{5}$$

for a normal mode $\mathbf{n_i}$ of vibration i of the isolated phenanthroline molecule. The corresponding normal mode of the phenanthroline-solvent-molecules complex is $\mathbf{m_i}$. Because the length of vector $\mathbf{m_i}$ is larger than the length of $\mathbf{n_i}$, those entries which correspond to the solvent molecule coordinates in $\mathbf{m_i}$ were removed, which is equivalent to adding zero entries to the smaller vector $\mathbf{n_i}$. This reduced normal mode, which must not be normalized, is denoted $\tilde{\mathbf{m}}_i$. Then, A^i_{mm} measures the contribution of collective motions of phenanthroline atoms to the total vibration in the solvent complex, while A^i_{nm} reveals the fraction of the mode $\mathbf{n_i}$ of well-defined symmetry species in the solvent-distorted (symmetry-reduced) mode $\tilde{\mathbf{m}}_j$. Results of this analysis are given for selected vibrations of the water-methanol complex of phenanthroline in Table 4. For low-frequency modes, the wavenumber shift $\Delta\tilde{\nu}_i$ correlates nicely with the A^i_{nm} measure, whereas no such correlation exists in the high-frequency regime. Mode numbers 4−7 show reduced contributions of the phenanthroline molecule to the total vibration of the hydrogen-bonded complex accompanied by a significant shift of the wavenumbers.

To conclude, the modeling of microsolvation in this cluster approach has demonstrated that the vibrations of solvent molecules with those of phenanthroline couple in those frequency ranges where Fermi resonances can occur. However, these couplings affect the wavenumbers only little and shifts are smaller than the range of error of the quantum chemical methods. Therefore, the discussion of the experimental spectra is indeed possible on the grounds of the isolated molecule calculation.

6. Conclusion

In this work, we have extensively revised the assignment of experimental vibrational bands of 1,10-phenanthroline polarized Raman spectra, which were recorded employing different solvents and crystalline material. The electronic structure of the molecule was modeled within a density functional framework using triple-ζ basis sets of different size. Raman intensities were calculated within the double harmonic approximation. As a result, a detailed picture of the vibrational motions of 1,10-phenanthroline emerges, which is of great value for understanding nuclear motions in transition metal complexes that involve phenanthrolines as ligands. In addition, a few corrections of earlier assignments are made.

A discussion of the accuracy of calculated Raman intensities was possible since all normal modes with sufficient intensity could be assigned uniquely. For 1,10-phenanthroline, we found a very satisfactory agreement of calculated and experimental Raman intensities. Even with the (moderately sized) TZVP basis set, which is a reliable standard basis set for structure optimizations and energy calculations, fairly accurate relative Raman cross sections were obtained. For much larger molecules than phenanthroline, the basis sets studied here may be used in taylored methods, which are, for instance, described in refs 27, 21, and 50 for the calculation of Raman spectra of molecules with 100 and more atoms.

With respect to the basis sets used in the quantum chemical calculations we summarize that Ahlrichs-type triple-ζ basis sets provide frequencies and Raman activities, which compare very well with experiment. In our semi-numerical approach, Sadlej's triple-ζ basis set does not yield accurate frequencies for out-of-plane vibrations, which are most affected by basis set superposition effects.

Acknowledgment. Financial support from the Fonds der Chemischen Industrie (FCI) and from the Deutsche Forschungsgemeinschaft DFG through the collaborative research center SFB 538 "Redoxaktive Metallkomplexe" is gratefully acknowledged.

References and Notes

(1) König, E.; Madeja, K. *Spectrochim. Acta* **1967**, *23A*, 45−54.
(2) König, E.; Madeja, K. *Inorg. Chem.* **1967**, *6*, 48−55.
(3) Gallois, B.; Real, J.-A.; Hauw, C.; Zarembowitch, J. *Inorg. Chem.* **1990**, *29*, 1152−1158.
(4) Sorai, M.; Seki, S. *J. Phys. Chem. Solids* **1974**, *35*, 555−570.
(5) Zimmermann, R.; König, E. *J. Phys. Chem. Solids* **1977**, *38*, 779−788.
(6) Bousseksou, A.; Constant-Machado, H.; Varret, F. *Phys. I France* **1995**, *5*, 747−760.
(7) Bousseksou, A.; McGarvey, J. J.; Varret, F.; Real, J. A.; Tuchagues, J.-P.; Dennis, A. C.; Boillot, M. L. *Chem. Phys. Lett.* **2000**, *318*, 409−416.
(8) Brehm, G.; Reiher, M.; Schneider, S. *J. Phys. Chem. A* **2002**, *106*, 12024−12034.
(9) Baranovic, G. *Chem. Phys. Lett.* **2003**, *369*, 668−672.
(10) Moliner, N.; Salmon, L.; Capes, L.; Muñoz, M. C.; Létard, J.-F.; Bousseksou, A.; Tuchagues, J.-P.; McGarvey, J. J.; Dennis, A. C.; Castro, M.; Burriel, R.; Real, J. A. *J. Phys. Chem. B* **2002**, *106*, 4276−4283.
(11) Coates, C. G.; Callaghan, P. L.; McGarvey, J. J.; Kelly, J. M.; Kruger, P. E.; Higgins, M. E. *J. Raman Spectrosc.* **2000**, *31*, 283−288.
(12) Ujj, L.; Coates, C. G.; Kelly, J. M.; Kruger, P. E.; McGarvey, J. J.; Atkinson, G. H. *J. Phys. Chem. B* **2002**, *106*, 4854−4862.
(13) Zgierski, M. Z. *J. Chem. Phys.* **2003**, *118*, 4045−4051.
(14) Perkampus, H.-H.; Rother, W. *Spectrochim. Acta* **1974**, *30A*, 597−610.
(15) Altmann, W.; Perkampus, H.-H. *Spectrochim. Acta* **1979**, *35A*, 253−257.
(16) Thornton, D. A.; Watkins, G. M. *Spectrochim. Acta* **1991**, *47A*, 1085−1096.

(17) Muniz-Miranda, M. *J. Phys. Chem. A* **2000**, *104*, 7803−7810.
(18) El Hajbi, A.; Vante, N. A.; Chartier, P.; Goetz-Grandmont, G.; Heimburger, R.; Leroy, M. J. F. *J. Electroanal. Chem.* **1986**, *207*, 127−150.
(19) Jang, N. H.; Suh, J. S.; Moskovits, M. *J. Phys. Chem. B* **1997**, *101*, 8279−8285.
(20) Zawada, K.; Bukowska, J. *J. Mol. Struct.* **2000**, *555*, 425−432.
(21) Reiher, M.; Neugebauer, J.; Hess, B. A. *Z. Physik. Chem.* **2003**, *217*, 91−103.
(22) Neugebauer, J.; Hess, B. A. *J. Chem. Phys.* **2003**, *118*, 7215−7225.
(23) Caillie, C. V.; Amos, R. D. *Phys. Chem. Chem. Phys.* **2000**, *2*, 2123−2129.
(24) Pecul, M.; Rizzo, A. *J. Chem. Phys.* **2002**, *116*, 1259−1268.
(25) Pecul, M.; Coriani, S. *Chem. Phys. Lett.* **2002**, *355*, 327−338.
(26) Neugebauer, J.; Reiher, M.; Hess, B. A. *J. Chem. Phys.* **2002**, *117*, 8623−8633.
(27) Neugebauer, J.; Reiher, M.; Kind, C.; Hess, B. A. *J. Comput. Chem.* **2002**, *23*, 895−910.
(28) Ahlrichs, R.; Bär, M.; Häser, M.; Horn, H.; Kölmel, C. *Chem. Phys. Lett.* **1989**, *162*, 165−169.
(29) Becke, A. D. *Phys. Rev. A* **1988**, *38*, 3098−3100.
(30) Perdew, J. P. *Phys. Rev. B* **1986**, *33*, 8822−8824.
(31) Schäfer, A.; Huber, C.; Ahlrichs, R. *J. Chem. Phys.* **1994**, *100*, 5829−5835.
(32) Dunning, T. H., Jr. *J. Chem. Phys.* **1989**, *90*, 1007−1023.
(33) Woon, D. E.; Dunning, T. H., Jr. *J. Chem. Phys.* **1994**, *100*, 2975−2988.
(34) Woon, D. E.; Dunning, T. H., Jr. *J. Chem. Phys.* **1993**, *98*, 1358−1371.
(35) Sadlej, A. J. *Collect. Czech. Chem. Commun.* **1988**, *53*, 1995.
(36) Sadlej, A. J. *Theor. Chim. Acta* **1991**, *79*, 123−140.
(37) Perera, S. A.; Bartlett, R. J. *Chem. Phys. Lett.* **1999**, *314*, 381−387.
(38) Ioannou, A. G.; Amos, R. D. *Chem. Phys. Lett.* **1997**, *279*, 17−21.
(39) McDowell, S. A. C.; Amos, R. D.; Handy, N. C. *Chem. Phys. Lett.* **1995**, *235*, 1−4.
(40) Kobayashi, R.; Koch, H.; Jørgensen, P. *Chem. Phys. Lett.* **1994**, *219*, 30−35.
(41) Eichkorn, K.; Treutler, O.; Öhm, H.; Häser, M.; Ahlrichs, R. *Chem. Phys. Lett.* **1995**, *240*, 283−290.
(42) Eichkorn, K.; Weigend, F.; Treutler, O.; Ahlrichs, R. *Theor. Chem. Acc.* **1997**, *97*, 119−124.
(43) Nishigaki, S.; Yoshioka, H.; Nakatsu, K. *Acta Crystallogr.* **1978**, *B34*, 875−879.
(44) Autschbach, J.; Ziegler, T. *Coord. Chem. Rev.* **2003**, *238*−*239*, 83−126.
(45) Long, D. A. *Raman Spectroscopy*; McGraw-Hill: New York, 1977.
(46) Amashukeli, X.; Winkler, J. R.; Gray, H. B.; Gruhn, N. E.; Lichtenberger, D. L. *J. Phys. Chem. A* **2002**, *106*, 7593−7598.
(47) Rabuck, A. D.; Scuseria, G. E. *Theor. Chem. Acc.* **2000**, *104*, 439−444.
(48) Reiher, M.; Sellmann, D.; Hess, B. A. *Theor. Chem. Acc.* **2001**, *106*, 379−392.
(49) Kirchner, B.; Reiher, M. *J. Am. Chem. Soc.* **2002**, *124*, 6206−6215.
(50) Reiher, M.; Neugebauer, J. *J. Chem. Phys.* **2003**, *118*, 1634−1641.